Rate Transitions in the Fatigue Crack Growth of Elastomers

I. C. Papadopoulos, A. G. Thomas, J. J. C. Busfield

Department of Materials, Queen Mary, University of London, Mile End Road, London E1 4NS, United Kingdom

ABSTRACT: It has been observed previously that cracks in elastomers under repeated strain initially grow rapidly from sharp cuts, but as the cracks proceed, the rate decreases to a steady value. This work examines these transitions from a sharp crack tip, introduced by a razor blade into a pure shear test piece, for a range of elastomers. The changes in the rate of crack growth are also reflected by changes in the fracture surface appearance, which roughens as the crack develops. This phenomenon is of practical significance in engineering applications, in which an initially fast crack growth rate from a sharp cut in a rubber product can result in significantly lower fatigue life than anticipated from the steady-state value, which is usually presented and quoted. The change in the rate with the number of cycles can be represented by an empirical relation whose parameters are functions of the strain energy release rate. The roughening of the crack can be envisioned as the splitting of a sharp tip into several tips with a consequent sharing of the strain energy release rate between them, leading to a reduction in the crack growth rates. This representation of the roughening process has been analyzed with a FEA approach. © 2008 Wiley Periodicals, Inc. J Appl Polym Sci 109: 1900–1910, 2008

Key words: elastomers; fatigue analysis; rubber

INTRODUCTION

Understanding fatigue crack growth propagation has become increasingly important in the rubber industry. Cyclic crack growth in elastomer components frequently leads to fatigue failure in which components fail at cyclic strain amplitudes much lower than their catastrophic tear strength as a result of cumulative cyclic fatigue crack growth. When cyclic crack growth is measured, the loading conditions and test piece geometries are often chosen so that the maximum strain energy release rate in each loading cycle is held constant throughout the test. With this approach, it is possible to measure the fatigue crack growth rate at specific strain energy release rates. Furthermore, the fracture surface roughness gives an indication of the average advancing crack tip radius that occurred during the fracture process.[1] As a result, the surface roughness is also thought to be a characteristic of the crack growth rate.

Busfield et al.[2] outlined the approach adopted in this article. Here, the energy required to drive the crack at a given rate is defined as the strain energy release rate, which is also sometimes known as the tearing energy (*T*):

$$T = -\left(\frac{\partial U}{\partial A}\right) \tag{1}$$

where *A* is the area of a single fracture surface of the crack and *U* is the total elastic strain energy stored in the component. The magnitude of *T* is mostly determined by the viscous work that has to be done in the crack tip region. Rivlin and Thomas[3] showed that the relationship between the crack growth rate and the strain energy release rate is a material property that is independent of the loading mode and specimen geometry.

Busfield et al.[4] showed that it is possible to predict the crack growth rates and the fatigue life of an engineering component. For the test pieces with an initial razor cut, the results were most accurate for cracks over 4 mm in length. At smaller crack lengths when the crack had not been fully roughened, the agreement between experimental and predicted data was not as good. This is probably due to the crack growth being faster from a sharp tip. Similar observations were made by Thomas,[1] Lake and Lindley,[5] and Lake and Yeoh,[6] who all reported that a sharp cut greatly accelerates the rate of crack growth per cycle during the first few loading cycles and that if the crack is kept artificially sharp by continuous cutting, the crack growth rate remains faster than that anticipated in the steady state. The initially torn surfaces nearest to the razor cut are called smooth growth, and the slower, steady-state condition is

Correspondence to: J. J. C. Busfield (j.busfield@qmul.ac.uk).

often called rough growth. The extent of this rapid transitory crack growth was reported to be within the range of 0.05–0.5 mm until the crack growth rate was more typical of the steady-state conditions at the specific strain energy release rate. Thomas[1] also proposed a mechanism to explain this reduction in the rate with an apparent roughening of the torn fracture surface. He proposed that if the roughened tip is assumed to consist of a number of small sharp tips, the value of the strain energy release rate for one of these will be less than for the tip as a whole by a certain factor and thus the crack growth rate will be reduced. This argument forms part of the investigation and is discussed in more detail here.

The kinetics of the roughening is the subject of the investigation described in this work. The cyclic crack growth was measured against the number of fatigue cycles for filled and unfilled natural rubber (NR) and styrene–butadiene rubber (SBR) materials for a range of strain amplitudes and hence different values of the strain energy release rate. This effect is of practical significance when roughening takes a significant fraction of the fatigue life, for example, when the crack growth rate is relatively high.

In actual fatigue processes, it is likely that the maximum strain energy release rate experienced during fatigue cycling might change either from cycle to cycle or from a large number of cycles at a small value to a smaller number of cycles at a higher strain energy release rate. It is possible that there may be some memory of the earlier lower crack growth rate. It is clear from work by Ratsimba[7] that the characteristic steady-state fatigue fracture surface roughness might take a number of cycles to develop. In a transition from small strain amplitudes to larger ones, it is likely that the initial crack growth rate might differ from the final steady-state rate. Therefore, this work also reports on experimental results for a cyclically loaded pure shear test piece for which the extent of transitory crack growth was measured between a small-amplitude (low strain energy release rate) and large-amplitude cyclic strain test (high strain energy release rate).

EXPERIMENTAL

Pure shear test

The relationships between the tear rate per cycle and the strain energy release rate were found to be geometrically independent by Rivlin and Thomas.[3] Similarly, the crack growth rate per cycle (dc/dN) has also been found to be a geometrically independent function of the strain energy release rate:

$$\frac{dc}{dN} = f(T) \qquad (2)$$
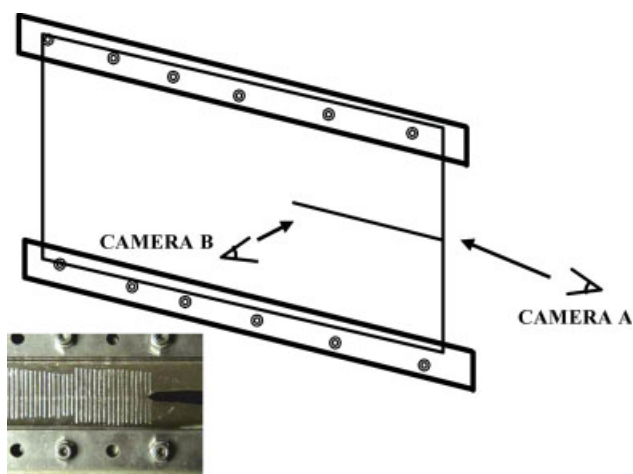
Figure 1 Schematic representation of the camera positions during the crack growth measurements of the pure shear specimen. [Color figure can be viewed in the online issue, which is available at www.interscience.wiley.com.]

where c is the crack length, N is the number of cycles, and T is the maximum strain energy release rate during the cycle. In this work, the crack growth rate was studied in the pure shear test piece shown in Figure 1 with the standard procedure described by Busfield and coworkers[2,4] and Papadopoulos et al.[8] The strain energy release rate for the pure shear test piece is given as follows:

$$T = Wl_0 \qquad (3)$$

where W is the strain energy density distant from the crack tip, which can be deduced from the strain in the pure shear region and knowledge of the pure shear stress/strain relationship. l_0 is the height of the pure shear test specimen.

An Instron 8801 servohydraulic machine (High Wycombe, UK) with a 1-kN capacity load cell at a frequency of 0.5 Hz for the SBR specimens and 1 Hz for the NR specimens was used for the experiments. The pure shear test pieces were strained to a maximum displacement between 5 and 70% and relaxed to zero strain in each cycle. The SBR specimens included unfilled SBR (SBR0), filled SBR with 10 parts of N330 carbon black per hundred parts of rubber (SBR10), and filled SBR with 50 parts of N330 carbon black per hundred parts of rubber (SBR50). The NR specimens included unfilled NR (NR0) and filled NR with 23 parts of N339 per hundred parts of rubber (NR23). The formulations and curing conditions for each formulation are given in Table I.

The test dimensions for the pure shear specimens were a length of 175 mm, a height of 24 mm, and a thickness of 2.0–2.5 mm. Before the crack growth testing, an initially 30-mm-long razor blade cut was introduced into the central axis of one edge of the test piece. The side of the test specimens was

TABLE I
Formulations of NR and SBR Materials

Ingredient (pphr)		NR0	NR23	SBR0	SBR10	SBR50
NR		100	100			
SBR				100	100	100
Carbon black	N330				10	50
	N339		23			
Sulfur		2.7	2.7	2	2	2
Stearic acid		2	2	2	2	2
Zinc oxide		5	5	3	3	3
Antioxidant HPPD		3	3	3	3	3
Accelerator	CBS	1.5	1.5			
	DPG			1	1	1
Cure temperature (°C)		145	160	160	160	160
Cure time (min)		50	3	45	40	40

HPPD, N-1.3-dimethylbutyl-N′-phenyl-p-phenylenediamine; CBS, N-cyclohexyl-2-benzothiazyl-sulfenamide; DPG, diphenyl guanidine.

marked with lines at constant intervals to assist with accurate measurements of the crack growth during the propagation. Also, a silver pen mark was made to define the edge of the crack tip. This was used to measure the initial propagation. To determine the crack growth rates, video cameras were used to capture images during the loading process.

Crack growth measurement

Two cameras were set up to monitor the propagation during the cyclic loading tests, as shown in Figure 1. One camera (A) was set to look into the crack tip from the end of the test piece during extension, and the other one (B) was set up perpendicular to the pure shear test piece to record the increase in the crack length of the propagating crack. As the specimen was cyclically extended during the test, tearing occurred locally at the tip of the crack. At small cyclic strains, it was not possible to measure the very small individual increments in each cycle accurately with camera B capturing images perpendicularly to the test piece. Therefore, in the initial stages of the fatigue test, images from camera A were used. For this, a single ink mark was made inside the crack tip profile, as the crack tip extended into fresh rubber; then, this mark was split into two, and the separation between these two marks indicated the extension of the crack, as shown in Figure 2. At the maximum extension, it is presumed that the rubber at the crack tip is stretched to about its limiting extension (λ_B); therefore, the distance that the cut has grown (Δc), referred to the unstrained state, is approximately given by

$$\Delta c = x/2\lambda_B \quad (4)$$

where x is a measure of the height of the freshly torn rubber at the tip. It can be measured from the

distance between the split mark at the tip. Still images from camera A were examined to determine distance x between the newly exposed edges at the crack tip. This technique was particularly good for measuring the initial crack growth rates. Once the crack had been cycled extensively, it was possible to monitor the average increase in the crack length per cycle with camera B alone.

First, the images from the camera looking into the crack tip were processed to acquire the initial rapid crack propagation. This technique gave the crack growth readings, which could not be readily captured with the traditional method of measuring from the side of the pure shear specimen when the growth per cycle is too small to be easily resolved. Once the crack had grown sufficiently long to be monitored from the side camera, then those images were employed. The growth measured from the first camera position required a minor scaling of about 10% so that consistent crack growth behavior at the camera changeover occurred. The adjustment involved the comparison of the last few crack length values measured with the camera looking into the crack tip and the first few captured from the side. The initial points were then multiplied by this small factor so that they were brought into line with the values measured along the profile with camera B once the crack had grown far enough to be reliably resolved. This discrepancy arose because the strain at the tip of the crack was slightly less than the breaking strain. To reduce errors, the videoed images were projected onto a screen to make the measurements more accurate.

Fracture surface microscopy

The analysis of the fracture surfaces and profiles could yield information on the characteristic crack growth rates. Optical microscopy was employed to study the fracture surfaces created during the cyclic loading tests at different strain energy release rates.
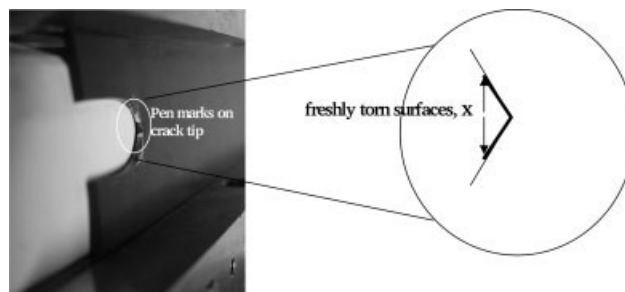

Figure 2 Photograph of the test piece taken from camera A and a schematic representing the tip of the crack during the initial cyclic loading.

Samples 5–10 mm in length were cut for microscopic examination from the fatigue test pieces with a razor blade. This length was adequate to view under the microscope a substantial fracture surface and therefore to differentiate between variations on the surface created by the different rates of propagation. The samples were mounted on a base, and the surfaces were observed through a Meiji EMZ-TR microscope (Meiji Techno UK, Ltd., Axbridge, UK) connected to a computer station equipped with Image-Pro Express software (Bethesda, MD).

Finite element analysis (FEA) of a pure shear model

The analysis of a two-dimensional pure shear model was carried out to compare the difference in the strain energy release rates for two situations in which it is assumed that the crack tip splits into two small tips propagating at an angle of $30°$ instead of the normal straight path. The first model involves two cracks of the same length growing at $30°$, as shown in Figure 3(a). The second model, which is illustrated in Figure 3(b), simulates a situation in which one of the crack tips (in this case the upper one) propagates further than the tip at the lower half of the pure shear model. This FEA exercise was carried out to assist with the understanding of the origins of the fracture surface roughness during the cyclic crack growth tests on the pure shear test pieces. This investigation is related to the suggestion by Thomas[1] that the crack tip might consist of a number of smaller tips, each with a fraction of the total strain energy release rate.

The models were created with the Ideas design package (SDRC, Stevenage, UK). The commercial finite element program ABAQUS (Providence, RI) (version 6.3.1) was used to calculate the energy release rate. In ABAQUS, several different large-strain hyperelastic materials models are available. This work used Yeoh's[9] stored energy function, whose coefficients were obtained from stress–strain data measured in tension for the materials modeled. The elements applied in the model consisted of plain stress CPS4 elements. The models were displaced by global extension ratios of 1.25 and 1.50. In this work, the energy balance technique,[10] in which the difference in the magnitude of the internal strain energy (dU) is calculated between two models held at a fixed displacement when the crack tip area (A) is extended by a small area (dA), was used to calculate the strain energy release rate, with the strain energy release rate being equal to $-dU/dA$. This technique is also sometimes known as the node release or virtual crack extension technique.
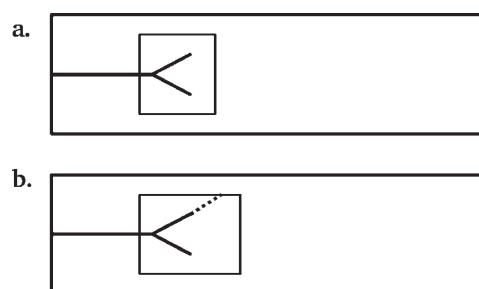
Figure 3 Schematic of the models of the crack tip of the pure shear test piece: (a) two cracks opening at $30°$ to the horizontal and (b) two cracks opening at $30°$ to the horizontal, with the upper crack extending further than the crack at the lower half of the model.

Elastomer materials

Busfield et al.[11] noted that the detailed fatigue crack growth mechanisms observed in SBR materials are different from those found in strain-crystallizing materials such as NR. In addition, Tsunoda et al.[12] showed that the addition of carbon black fillers also has a significant effect on the rates of both tearing and fatigue crack growth. As a result of these observed differences, both NR and SBR materials are investigated here with and without the incorporation of carbon black.

RESULTS

Measurement of the rate of crack propagation

A general trend was observed for the change in the rate of crack propagation for cracks initiating from a sharp, artificially inserted blade cut. The initial crack growth rate was significantly faster than the steady-state fatigue crack growth rate. Figure 4 plots two typical graphs of crack growth versus the number of fatigue cycles from initially razor-cut samples for NR23 and SBR10. Clear transitions similar to those shown were apparent for all the tests, regardless of the maximum strain energy release rate in the cycle, with the crack growth rate eventually slowing down and reaching a steady-state condition under cyclic loading.

Figure 5 shows plots of the steady-state fatigue crack growth rate, which is defined as $R = (dc/dn)$ at different strain energy release rates for all five compounds. R represents the experimentally measured steady-state rate of propagation. It is the transition from the initially fast rate to the steady-state rate that is of interest in this work.

Microscopic investigation of crack surfaces

The examination of the fracture surfaces revealed information regarding the nature of the crack propaga-
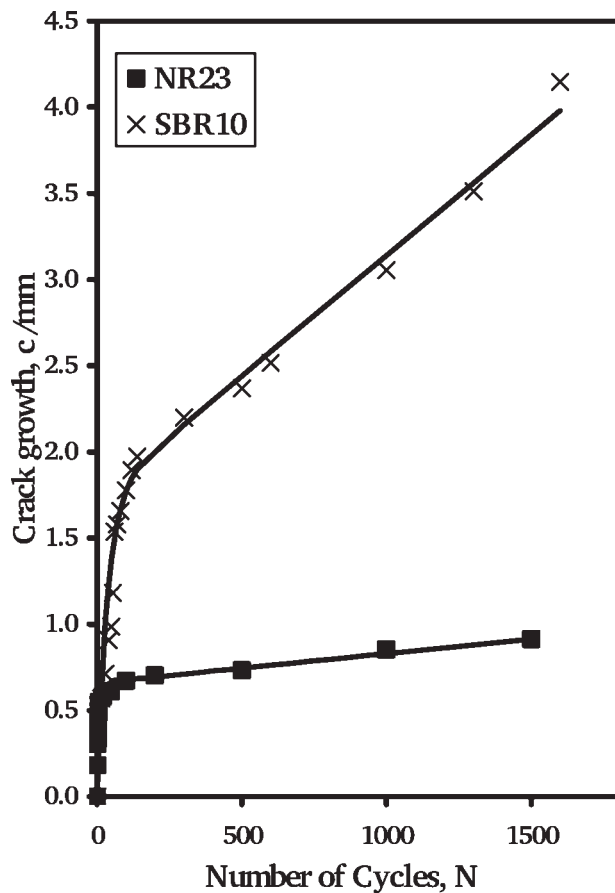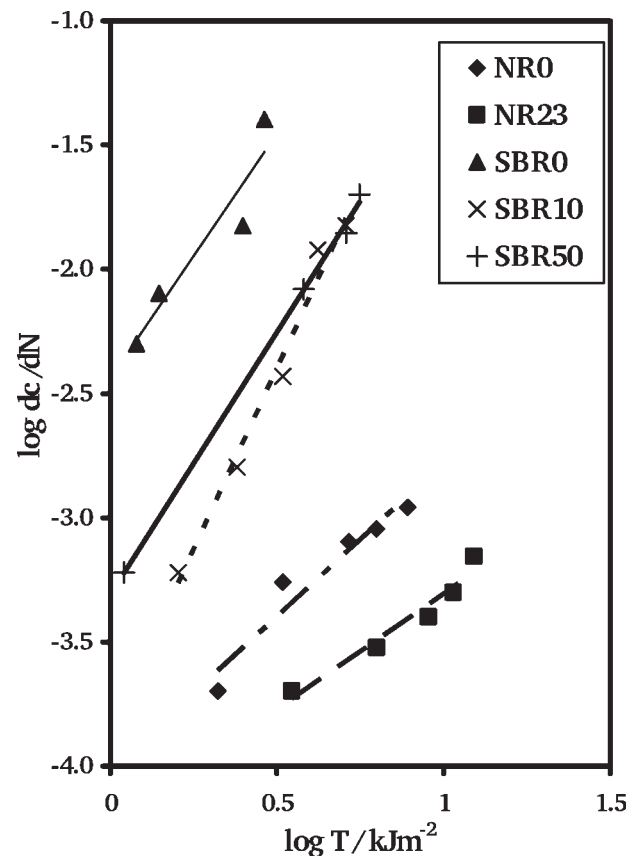
Figure 4 Illustration of the dynamic crack growth curve for NR23 ($T = 3.4$ kJ/m^2) and SBR10 ($T = 2.4$ kJ/m^2). The measured data are shown as well as the best fit function given by eq. (6) for each data set.

Figure 5 Double log plot of dc/dN versus T for the five different materials.

tion in terms of velocity of propagation as well as differences in the crack growth depending on the inhomogeneity of the material under investigation. In the materials used in this work, the most obvious difference was the presence (or absence) of carbon black filler particles.

Microscopic images of the fracture surfaces and profiles of these surfaces resulting from the cyclic crack growth are shown in Figures 6–8. The fracture surfaces show the different regions resulting from the high growth rate and the steady-state rate for the different tests. The fracture surface microscopic images were taken with the instrument looking down onto the fracture surface, and the profiles were microscopic images taken across the width of the test pieces.

The NR materials showed a very clear transition from a fast crack growth rate from the razor-cut edge to a slower, steady-state rate. The change in the rate of propagation was accompanied by a change in the appearance of the crack surface from an initially smooth surface to a rough surface at a steady-state crack growth rate. Figures 6–8 show typical fracture
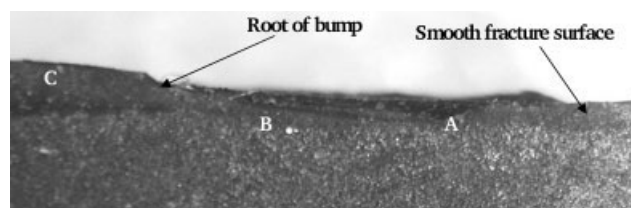
surfaces and profiles of the materials under investigation. For the NR materials, the difference in the appearance of the fracture surface was easily appa-
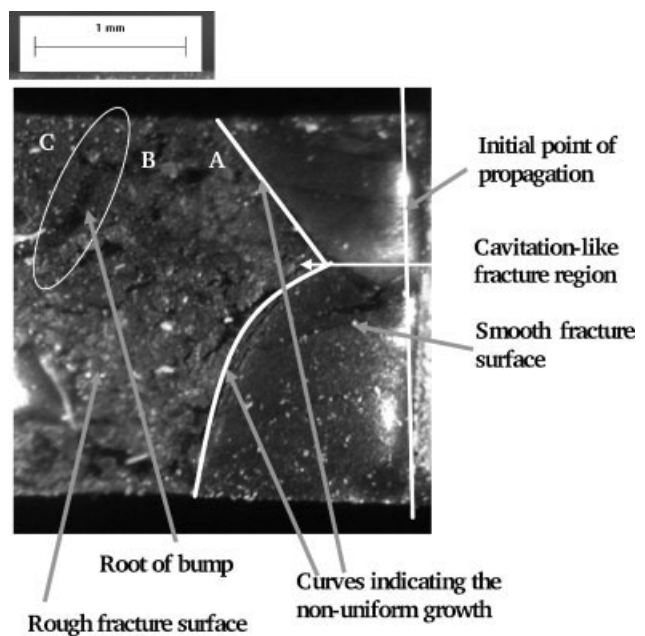
Figure 6 Fracture surface of NR23 at $T = 12.3$ kJ/m^2 indicating the regions of interest.

Figure 7 Profile of the fracture surface with labels of corresponding regions.

rent as the surface became rougher. Andrews[13] described this roughness as a region in which fracture can be seen to have propagated on different levels over small areas of the surfaces.

In Figures 6 and 7, several characteristic features of the growth during the transition can be identified. Initially, the growth is accompanied by a distinctly smooth surface, which is not uniform in its growth. The curves drawn on the fracture surface of Figure 6 highlight the region in which this behavior takes place. As the crack grows further, the surface becomes rougher, and there a steplike transition occurs into a different level of surface roughness with many larger bumps and depressions. A characteristic "depression" is shown as label A on Figures 6 and 7, and a "bump" is shown in the circled area of the rough surface, where the peak is labeled C.

In all of the fracture surfaces for NR0, examples of which are shown in Figure 8, there is an initially smooth fracture region close to the sharp cut that corresponds to the initially fast rate of propagation. On the $T = 2.1$ kJ/m^2 fracture surface, the transition to a rough region was achieved over a shorter distance in comparison with tests at higher values of T. A closer examination of the edge profiles shows that the transition at $T = 2.1$ kJ/m^2 results in a lower surface roughness in the steady state in comparison with the higher values of T.
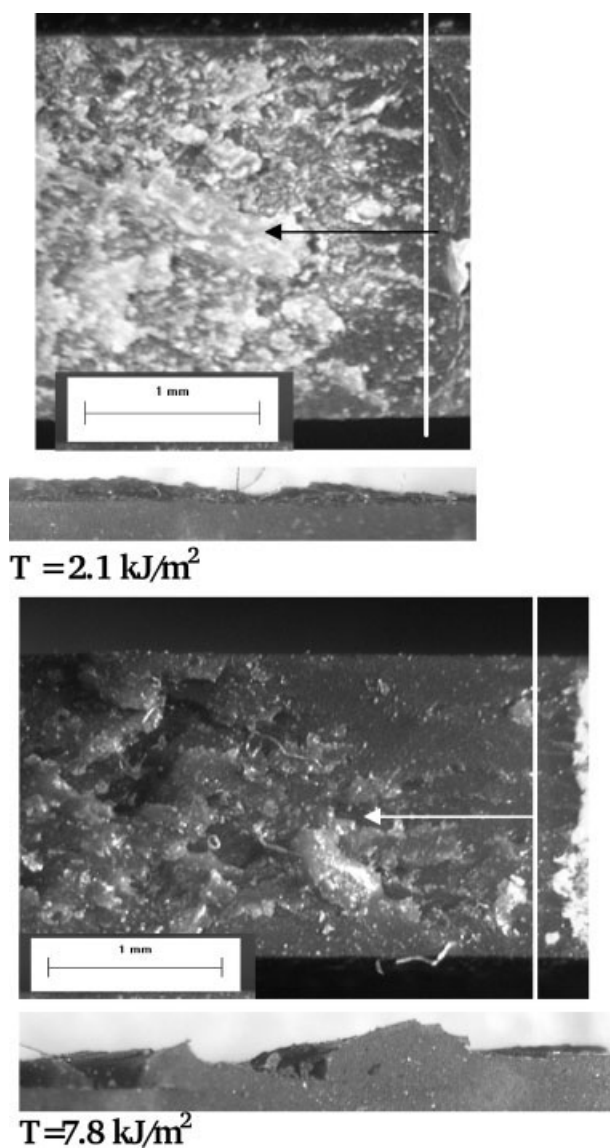
The roughness of the fracture surfaces of the higher T tests on NR0 was, in contrast, substantially greater. Comparing the low T profiles to the mid and high T profiles, one can safely conclude that the rough surfaces are different in morphology in terms of the depth of the depressions. The higher T is, the faster the propagation is and the greater the roughness is of the fracture surface in the steady state. This observation is in agreement with previous research by Thomas,[1] Andrews,[13] and Lake and Yeoh,[6] who all reported that slow fracture accompanies smoother surfaces and rapid fracture gives rise to rougher ones.

The introduction of the filler into the NR23 material reinforced the tear strength of the material; therefore, the steady-state crack growth rate was slower than that of NR0. There was also a transition from a smooth surface to a rough fracture surface.

The test piece at lower values of T had a shorter smooth surface region in comparison with a test piece at a higher value of T, at which the transition was more distinct. Again, observation of the profile of these fatigue fracture surfaces reveals that low T values give smoother surfaces than higher T values.

A common feature of all the fracture surfaces of the NR materials is faster growth into the rough surface in the center of the test pieces. This feature is shown clearly in Figure 6 for NR23 on the $T = 12.3$ kJ/m^2 fracture surface, which is the area within the curves. An attempt to explain possible reasons for this behavior in NR materials forms part of the discussion.

During the cyclic tests on the SBR materials, crack propagation in the first few cycles was occasionally

Figure 8 Fracture surfaces and profiles of the surfaces of NR0 test pieces indicating the dependence of the degree of roughness on T. The arrows indicate the direction of crack growth.

accompanied by distinct "jumps" at the maximum strain during a cycle. At the high strain energy release rate values, this is a phenomenon similar to the observations by Lake and Yeoh,[6] who found that the crack with a very sharp tip propagated in an abrupt "jump". However, in cyclic loading, these were of smaller length. It was apparent that initially substantial crack growth was occurring in a single cycle instead of more uniform growth over a number of cycles, as observed in the NR materials. However, in general, just as with the NR materials, the initial crack growth rate from the razor cut was again significantly faster than the steady-state fatigue crack growth rate.

In the SBR fracture surfaces, the transition from a smooth surface to a rough fracture surface was less apparent. However, a careful examination of the profiles of the fatigue fracture surfaces again reveals that greater depth variations occur at higher strain energy release rates.

The sections that follow discuss several arguments for a better understanding of these transition phenomena.

Mathematical representation of the crack growth behavior

The crack growth initiating from a sharp cut is significantly faster in comparison with the eventual rate reached at the steady state. In this work, an attempt was made to quantify the transition change in terms of the crack length (mm) and the number of cycles. Figure 4 shows two experimental cyclic crack growth data sets, one for NR23 at $T = 3.4$ kJ/m^2 and the other for SBR10 at $T = 2.4$ kJ/m^2. Both data sets were typical of all the materials examined. The steady-state rate of propagation was described as follows:

$$c = RN \qquad (5)$$

where R is the steady-state fatigue crack growth rate per cycle for the particular material measured at a specific value of T, as shown in Figure 5. The rate transition region was readily fitted with the following expression:

$$c = RN + c_0 \left(1 - \exp\left(-\frac{N}{N_0}\right)\right) \qquad (6)$$

where c_0 is the amount of additional crack growth that would not be predicted if only the steady-state behavior were considered. The value of N_0 is a characteristic of the specific transition being measured and is related to the number of cycles that are required for the steady state to be achieved. The lines shown in Figure 4 were fitted with this equa-
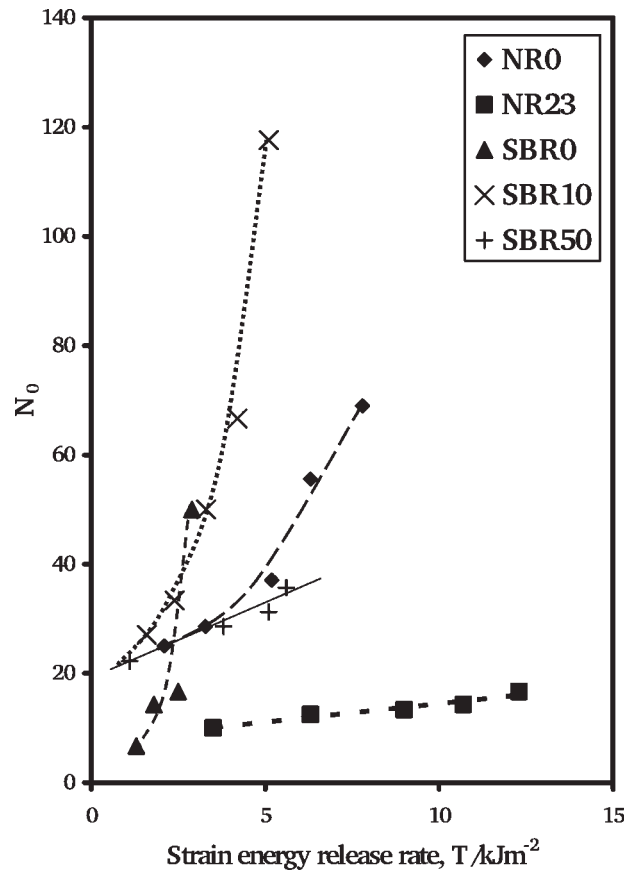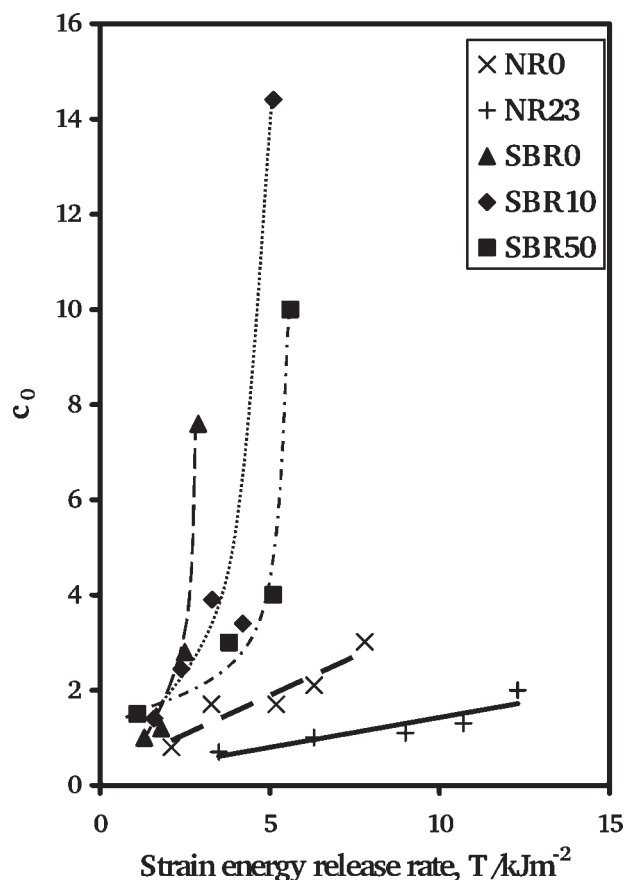
Figure 9 Variation of N_0 with T for different tear rate transitions for NR and SBR materials.

tion to derive the appropriate values for c_0 and N_0. This fitting process was followed for a wide range of different transitions and was seen to give excellent agreement for all the cases examined in this article. The relationship between N_0 and the strain energy release rate value for each material is shown in Figure 9, and the relationship between the length of the transition zone (c_0) and the strain energy release rate is shown for all the materials in Figure 10.

In general, both c_0 and N_0 increase with T for all the materials examined. In NR0, the values of c_0 and N_0 are greater than those for the filled material (NR23), and hence the transitions are slower (more cycles and longer crack growth). This could be associated with the crack path deviation being introduced more readily because of the presence of the filler, which may cause the fracture surface to roughen up more rapidly. The value of N_0 is also much less dependent on the maximum strain energy release rate for the filled NR.

Variation of the growth rate with a changing strain energy release rate

The aim of this part of the work was the study of the extent of the transitory crack growth with T

**Figure 10** Variation of c_0 with T for different tear rate transitions for NR and SBR materials.

changing during the test. The applied technique is similar to that used for monitoring transitions from a blade cut. Cyclic fatigue crack growth tests were undertaken at specific maximum displacement amplitudes on pure shear specimens until steady-state conditions were established. The amplitude was then altered, and the fatigue crack growth rate was measured continuously until steady-state crack growth rate conditions were again attained. The tests were conducted with both the NR0 and NR23 compounds. Representative results are shown in Figures 11 and 12. There was a general transition trend with the strain energy release rate changing as shown. In all of these cases, more rapid crack growth occurred before the crack propagation settled to steady-state growth for the particular T value. These faster initial crack propagations were probably a result of an initially sharp effective crack tip profile from the previous low strain energy release rate test; this was sharper with respect to the steady-state crack tip at the high strain energy release rate. This sharper crack tip prevailed for a few hundred or thousand cycles (at low T) after the larger amplitude cyclic strains were applied, producing a higher crack growth rate. It was not surprising that these differ-

ences between the initial and steady-state cyclic crack growth rates also appeared to be more pronounced the greater the difference was between the low and high strain energy release rate magnitudes. These tests showed that the extent of the transitory crack growth was between a few hundred and few thousand cycles, so it should be noted that tests lasting significantly longer that a few thousand cycles should be used to condition a test piece before the steady-state crack growth rate is recorded for a given strain energy release rate.

The phenomenon is discussed in the next section with respect to the findings of the rest of the experimental work.

DISCUSSION

It has been shown in the experimental results that a crack propagates faster when the tip is not blunted (initial rate of propagation), and a sharp tip will create a relatively smooth fracture surface until it reaches a steady-state rate, at which the crack surfaces becomes rougher. This was evident especially in the NR cyclic tests. Furthermore, in all five compounds of NR and SBR tested, the higher strain energy release rate tests were accompanied by a
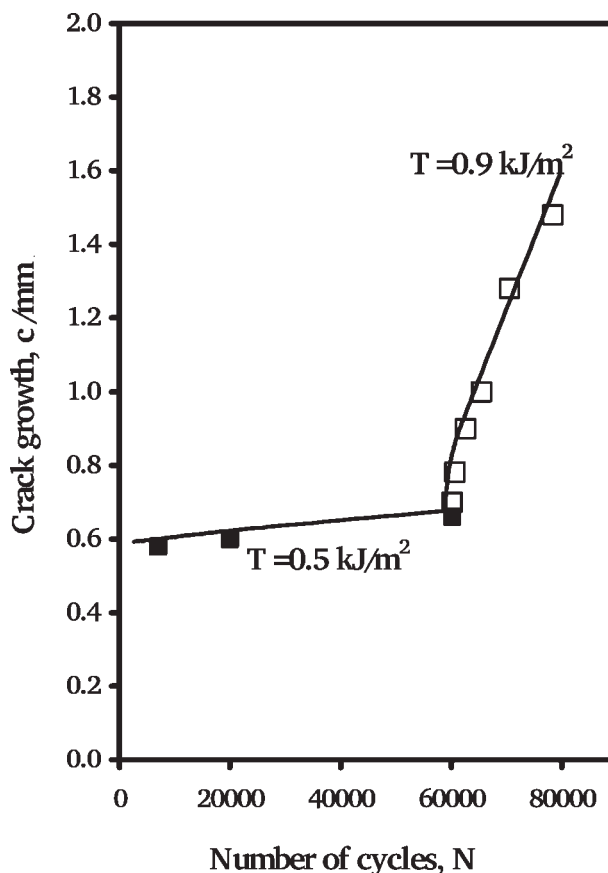
Figure 11 A low to high strain energy release rate transition in NR0.
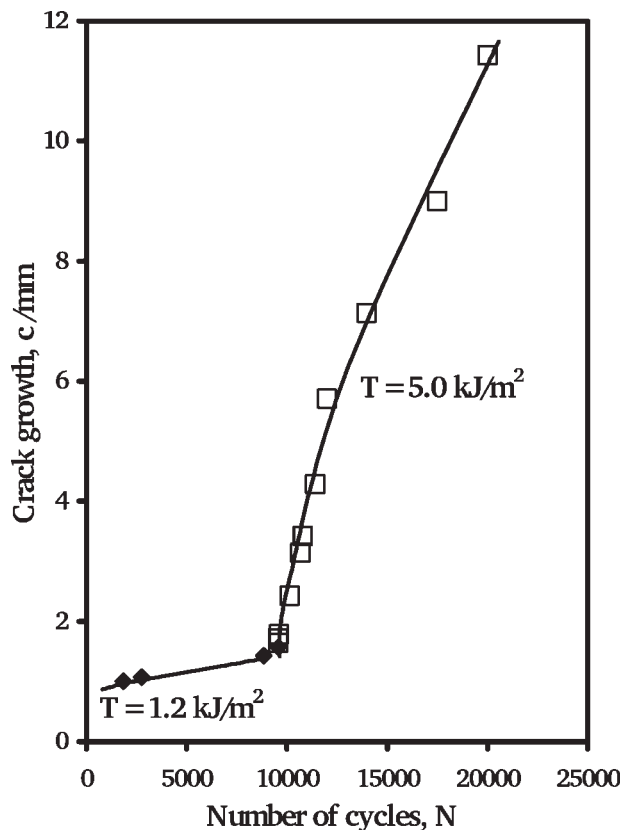
Figure 12 A low to high strain energy release rate transition in NR23.

higher degree of roughness in the steady-state region of propagation. Thomas[1,14] argued that for NR materials irregularities develop at the crack tip during the loading history. These irregularities may act by increasing the effective crack tip radius and thus lowering the strain concentration there. This discussion attempts to explain the phenomena that occur during these transitions by considering the changes in morphology in the crack tip and fracture surfaces.

Anisotropy of a highly strained material near the crack tip is a likely factor for the change in roughness of the fracture surface during the cyclic crack growth tests. The surface roughness at equivalent T values was greater for the NR compounds than the SBR materials. This most likely resulted from the anisotropy being greatest in the NR compounds as a result of strain-induced crystallization. The differences in strength in different directions induced under large deformations were investigated by Busfield et al.[2] They reported that the high degree of polymer orientation that results from large strains can lead to an advancing crack profile spontaneously deviating from the anticipated path, which is at right angles to the maximum principle tensile stress field. This causes an effective blunting of the crack tip that may be responsible for the initially smooth crack surface, initiating from the sharp blade cut tip, changing into

a rough surface. Lake[15] commented that large reductions in tear strength were found in the direction of a moderate prestrain for filled and unfilled NR and SBR materials. In the cyclic crack growth carried out in this work, there were no prestrain conditions; however, Gent and Kim[16] reported induced anisotropy in strength even after the removal of the prior extension in carbon black filled NR compounds. This behavior could lead to the tendency for cracks to branch or deviate from the "plane" of propagation, creating a rough surface. The occurrence of branching is much more likely at higher strain energy release rates.

Thomas[1] proposed an alternative description of the change to a rough surface for a propagating crack. He suggested that the roughened tip consists of a number of small sharp tips, the value of T for each being less than that for the tip as a whole. To investigate the validity of this proposed theory, a simple two-dimensional, half-symmetry pure shear model was used to compare T for two different scenarios of crack tip branching.

The energy balance approach [eq. (1)] was used to calculate T at the crack tips. Here the change in the internal strain energy was calculated between two models held at a fixed displacements of global extension ratios of 1.25 and 1.50, at which the crack tip area was extended by a fixed area. Table II shows the comparative results of the finite element (FE) models at global extensions ratios of 1.25 and 1.50 in direction 2. The particular values for the global extension ratios in the FEA were chosen from the experimental part of this work and represent the values required to produce crack growth surfaces with roughness in the case of the 1.25 extension ratio and high surface roughness at a global extension ratio of 1.50.

In the FE models involving propagation at +30 and $-30°$, the local strain energy release rate for each tip is compared to the calculated global strain energy release rate for the pure shear model. In the case of the two cracks propagating at +30 and $-30°$

TABLE II
Values of T at Global Extensions of 1.25 and 1.50 for a Pure Shear Model

Crack direction		Global extension	
		1.25	1.50
a ⟶	$T = Wl_0$	2.09 kJ/m^2	7.10 kJ/m^2
b ⟨	$T = Wl_0$	2.09 kJ/m^2	7.10 kJ/m^2
	FEA calcd	1.02 kJ/m^2	3.41 kJ/m^2
c ⟨	$T = Wl_0$	2.09 kJ/m^2	7.10 kJ/m^2
	FEA calcd	1.61 kJ/m^2	4.76 kJ/m^2

[a] At 0° to the horizontal direction.
[b] Two cracks growing at 30° to the horizontal.
[c] Two cracks growing at 30° to the horizontal: one of the cracks propagates further in the same direction.

to the perpendicular direction of the applied extension ratio of 1.50, the strain energy release rate at each crack tip is 3.41 kJ/m^2. Therefore, if the crack tip splits into two equal cracks as a result of strain-induced anisotropy in the region of the crack tip, then the total strain energy release rate could be the sum of all the strain energy release rates for all the cracks in the model. The same argument is valid for the case of the 1.25 global extension ratio model, although the strain energy release rate is of a smaller magnitude ($T = 1.02$ kJ/m^2). The fact that T on each tip is slightly less than half of the global T value suggests that if the anisotropy that caused the crack front to split in the first place were removed, then there would be a tendency for the cracks to move back into a direction at 0°.

Opening just one of the tips further, that is, increasing the crack length in one of the two small tips, involved a higher local strain energy release rate in the opening crack than when both of the two equal cracks propagated. In the case of the 1.50 global extension ratio, the strain energy release rate was 4.76 kJ/m^2, and for the 1.25 global extension ratio, the strain energy release rate was 1.61 kJ/m^2. The higher T for the single tip propagating further suggests that once one of the tips becomes shorter than the other, it becomes shielded, and the other moves faster. The shielded crack tip has a decreasing strain energy release rate, which could suggest that eventually the crack growth in the region of this tip is "arrested" when the value drops to virtually zero.

This behavior might be a likely explanation for the higher degree of roughness at high values of the strain energy release rate. At small strains, the probability of a crack deviating is smaller because the individual T values are smaller and thus the crack will not bifurcate as readily. Once bifurcated, the cracks both extend until one becomes long enough to shield the other. At a higher global T value, this requires the "arrested" crack to travel further before the strain energy release rate value drops to a value near zero. The resulting longest extended crack tip might then change back to the forward direction where the strain energy release rate is higher. As an elementary tip grows beyond the shielding effect of its neighboring tip, the larger anisotropy that is experienced causes the longer crack to bifurcate and thus produce a slower crack growth rate, allowing other elementary crack tips to catch up. This process is repeated cyclically. Thus, the cyclic crack growth exhibits a large variation in rates when measured from cycle to cycle.

The presence of the filler changes the tear behavior of the elastomer and, as a result, the morphology of the fracture surfaces. Filler particles are known to increase the resistance to tearing. The orientation of the particles at the tip is likely to produce not only an increased resistance to fracture in the forward direction but also weakened paths transversely. In filled materials, the creation of a rough surface during the cyclic crack growth propagation is caused by the presence of the filler, which causes deviations of the propagating crack from its original primary path. Fillers tend to increase the scale of the roughening phenomenon, which is evident in the results of this work. The fatigue profiles of the fracture surfaces of filled elastomers have more distinct peaks and depressions in comparison with the unfilled fracture surfaces. These features could be detected even with the naked eye, and larger variations were evident at the higher strain energy release rates.

Lake and Yeoh[6] characterized the crack growth in a test piece containing a sharp tip as small-scale tearing because, as they reported, the propagation represents a rapid, catastrophic failure on a relatively large scale. This small-scale tearing implies a propagation step or "jump" in the range of 0.05–0.5 mm. In this work, however, the phenomenon of crack growth initiating from an artificially sharp tip is considered to occur in a progressive rather than abrupt manner. The common feature in both investigations is the effect of the sharp tip on the fracture surface created and the tip blunting that occurs during the cyclic loading. They also suggested that a factor for the tip blunting during cyclic crack propagation involves the hydrostatic component of the tensile stress, which might be sufficient to cause cavitation in front of the advancing crack tip. One supporting observation is that the secondary fractures can occur at some distance from the main fracture plane. However, as yet unpublished independent observations made by the authors on transparent rubber do not show any obvious sign of cavitation occurring. These secondary fractures appear to be different fracture planes that recombine as the crack proceeds. Lake and Yeoh[6] reported that in the NR materials, the crack from the initial blade cut propagated in a non-uniform path across the test piece. The center of the crack reached a rough surface in a shorter distance in comparison with the outer sides of the crack. This could be attributed to "cavitation-like" fracture at the center of the test piece during the loading because of complex stresses in this region in comparison with stresses along the sides, which are closer to the condition of plane stress and which continue to have smooth crack surfaces for a greater distance than the crack center. This feature is not so obvious in the SBR fracture surfaces.

In addition to the pure shear tests with cracks initiating from sharp crack tips, work was presented on pure shear NR test pieces to investigate the transition in the rate of propagation when T was changing. It could be argued that the faster rate of propagation during the initial stages of higher

T values was caused by the sharper crack tip from the previous lower strain energy release rate because the lower T value would produce a relatively sharp crack tip in comparison with the steady-state rate at a higher strain energy release rate. The multiple-tip concept suggested earlier could again apply to the initially faster growth during a change to a higher value of T. During the low T test, the crack tip remains relatively sharp, and branching and formation of secondary cracks are limited. On a change to a higher T value, the crack tip may have a ''memory'' of the sharper crack tip, and therefore the crack propagates faster initially before eventually reaching a steady-state rate at which presumably a greater number of small tips exist.

These transitional rates of propagation were not visible in all the tests carried out. In the SBR materials, it was not always possible to observe changes in the rate of propagation when T was changing. For the NR materials, the transitions were more apparent during tests in which the strain energy release rate values were substantially different in magnitude. The transitions in these cases normally took place within 2000 cycles. These tests have particular significance in cyclic crack growth work because research carried out in this field frequently involves edge-cut test pieces. In this test piece geometry, the relation between the strain energy release rate and the crack length is given as follows:

$$T = 2kWc \quad (7)$$

As the strain energy release rate (T) is dependent on the crack length (c), then even if the amplitude of the maximum strain per cycle is kept constant, the strain energy release rate increases with the crack length. Therefore, it is likely that the surface roughness may not reflect the instantaneous value of the measured T value. This is because the roughness has been shown not to change instantly and depends on the previous tearing history.

CONCLUSIONS

The strain energy release rate (T) was used as the variable to characterize the cyclic fatigue crack growth behavior of various rubber materials. Although the behavior of the materials studied varied quantitatively, the general trend of the rate of crack propagation slowing down from an initially faster rate when the crack is grown from a sharp cut is the same for all materials.

From this work, it is apparent that the initial rate of propagation is substantially higher. However, under cyclic loading for all the elastomers examined here, the crack tip reaches a steady-state rate with a particular value according to Lake and Yeoh[6] for the effective crack tip diameter and for the roughness of the fractured surfaces. This is a characteristic of the material and of the particular strain energy release rate. Therefore, when it eventually reaches this steady state, the rate is approximately constant and slower.

For all cases of both unfilled and filled NR and SBR materials that are considered here, it is apparent that the comparison with experiments shows that eq. (6) provides a reliable way of analyzing these transitions and would be applicable for characterizing the initially very rapid non-steady-state fatigue crack growth resulting, for example, from the penetration of sharp objects into rubber components.

For both NR and SBR materials, the presence of reinforcing fillers facilitates the roughening of the fracture surfaces.

Strain-induced anisotropy is thought to produce the crack tip splitting under strain, and hence the extent of splitting on average determines the crack tip radius in the steady state and the final roughness of the fractured surfaces. The surface roughness in the steady state was greater for the NR compounds than the SBR materials. This most likely resulted from the anisotropy being greatest in the NR compounds as a result of strain-induced crystallization.

As an elementary tip grows beyond the shielding effect of its neighboring tip, the larger anisotropy that is experienced causes the longer crack to bifurcate and thus produce a slower crack growth rate, allowing other elementary crack tips to catch up. This process is repeated cyclically. Thus, the cyclic crack growth exhibits a large variation in rates when measured from cycle to cycle.

References

1. Thomas, A. G. J Polym Sci 1958, 31, 467.
2. Busfield, J. J. C.; Ratsimba, C. H. H.; Thomas, A. G. J Nat Rubber Res 1997, 12, 131.
3. Rivlin, R. S.; Thomas, A. G. J Polym Sci 1953, 10, 291.
4. Busfield, J. J. C.; Jha, V.; Liang, H.; Papadopoulos, I. C.; Thomas, A. G. Plast Rubbers Compos 2005, 34, 349.
5. Lake, G. J.; Lindley, P. B. J Appl Polym Sci 1964, 8, 707.
6. Lake, G. J.; Yeoh, O. H. J Polym Sci Part B: Polym Phys 1987, 25, 1157.
7. Ratsimba, C. H. H. Ph.D. Thesis, Queen Mary University of London, 2000.
8. Papadopoulos, I. C.; Liang, H.; Busfield, J. J. C.; Thomas, A. G. In Constitutive Models for Rubber III; Busfield, J. J. C.; Muhr, A., Eds.; A. A. Balkema: Lisse, The Netherlands, 2003; p 33.
9. Yeoh, O. H. Rubber Chem Technol 1990, 63, 792.
10. Busfield, J. J. C.; Davies, C. K. L.; Thomas, A. G. Prog Rubber Plast Technol 1996, 12, 191.
11. Busfield, J. J. C.; Tsunoda, K.; Davies, C. K. L.; Thomas, A. G. Rubber Chem Technol 2002, 75, 643.
12. Tsunoda, K.; Busfield, J. J. C.; Davies, C. K. L.; Thomas, A. G. J Mater Sci 2000, 35, 5187.
13. Andrews, E. H. J Mech Phys Solids 1963, 11, 231.
14. Thomas, A. G. J Polym Sci 1955, 18, 177.
15. Lake, G. J. Rubber Chem Technol 1995, 68, 435.
16. Gent, A. N.; Kim, H. J. Rubber Chem Technol 1978, 51, 35.